The risk of platelet activation can be calculated

A novel computational fluid dynamics approach for the estimation of platelet activation risk has been developed at National Medical Research Center for Hematology by the group of Prof. Georgy Th. Guria in collaboration with scientists from Moscow Institute of Physics and Technology.

Denis Pushin, researcher at the Laboratory of Mathematical Modeling of Biological Processes at the National Medical Research Center for Hematology, Tatiana Salikhova, a trainee researcher.

Platelet activation in high shear flow heightens the risk of arterial thrombosis. The activation can be initiated as a result of the action of suprathreshold shear stress on platelets. In the recent paper published in PLOS ONE journal authors have presented a novel numerical method for the analysis of platelet activation risk in large vessels.

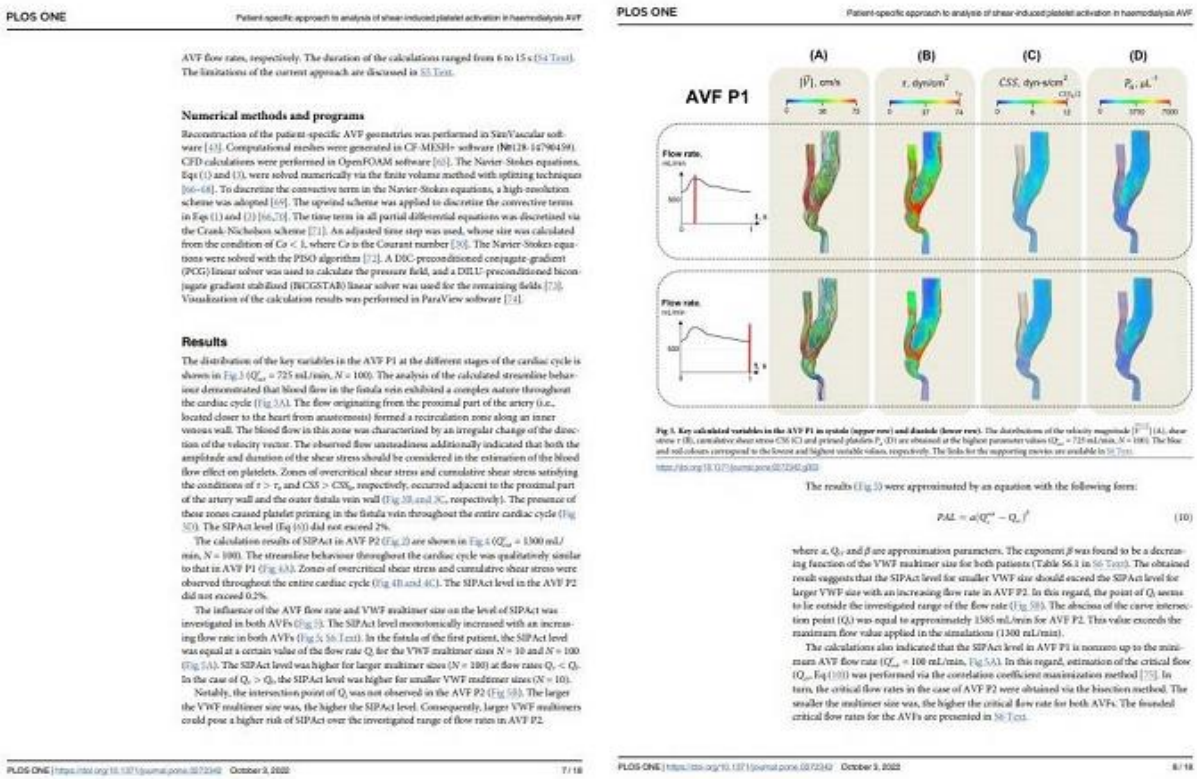

PLOS ONE

Patient-specific approach to analysis of shear-induced platelet activation in haemodialysis AVF

AVF flow rates, respectively. The duration of the calculations ranged from 6 to 15 s (S4 Text). The limitations of the current approach are discussed in S5 Text.

Numerical methods and programs

Reconstruction of the patient-specific AVF geometries was performed in SimVascular software [43]. Computational meshes were generated in CF-MESH+ software (Nt128-14790459). CFD calculations were performed in OpenFOAM software [65]. The Navier-Stokes equations, Eqs (1) and (2), were solved numerically via the finite volume method with splitting techniques [66–68]. To discretize the convective term in the Navier-Stokes equations, a high-resolution scheme was adopted [69]. The upwind scheme was applied to discretize the convective terms in Eqs (1) and (2) [66,70]. The time term in all partial differential equations was discretized via the Crank-Nicholson scheme [71]. An adjusted time step was used, whose size was calculated from the condition of $Co < 1$, where Co is the Courant number [36]. The Navier-Stokes equations were solved with the PISO algorithm [72]. A DIC-preconditioned conjugate-gradient (PCG) linear solver was used to calculate the pressure field, and a DILU-preconditioned biconjugate gradient stabilized (BiCGSTAB) linear solver was used for the remaining fields [73]. Visualization of the calculation results was performed in ParaView software [74].

Results

The distribution of the key variables in the AVF P1 at the different stages of the cardiac cycle is shown in Fig 3 (Q^{in}_{av} = 725 mL/min, N = 100). The analysis of the calculated streamline behaviour demonstrated that blood flow in the fistula vein exhibited a complex nature throughout the cardiac cycle (Fig 3A). The flow originating from the proximal part of the artery (i.e., located closer to the heart from anastomosis) formed a recirculation zone along an inner venous wall. The blood flow in this zone was characterized by an irregular change of the direction of the velocity vector. The observed flow unsteadiness additionally indicated that both the amplitude and duration of the shear stress should be considered in the estimation of the blood flow effect on platelets. Zones of overcritical shear stress and cumulative shear stress satisfying the conditions of $\tau > \tau_c$ and $CSS > CSS_{lin}$, respectively, occurred adjacent to the proximal part of the artery wall and the outer fistula vein wall (Fig 3B and 3C, respectively). The presence of these zones caused platelet priming in the fistula vein throughout the entire cardiac cycle (Fig 3D). The SIPAct level (Eq (6)) did not exceed 2%.

The calculation results of SIPAct in AVF P2 (Fig 2) are shown in Fig 4 (Q^{in}_{av} = 1300 mL/min, N = 100). The streamline behaviour throughout the cardiac cycle was qualitatively similar to that in AVF P1 (Fig 4A). Zones of overcritical shear stress and cumulative shear stress were observed throughout the entire cardiac cycle (Fig 4B and 4C). The SIPAct level in the AVF P2 did not exceed 0.2%.

The influence of the AVF flow rate and VWF multimer size on the level of SIPAct was investigated in both AVFs (Fig 5). The SIPAct level monotonically increased with an increasing flow rate in both AVFs (Fig 5; S6 Text). In the fistula of the first patient, the SIPAct level was equal at a certain value of the flow rate Q_c for the VWF multimer sizes N = 10 and N = 100 (Fig 5A). The SIPAct level was higher for larger multimer sizes (N = 100) at flow rates $Q_c < Q_c$. In the case of $Q_c > Q_c$, the SIPAct level was higher for smaller VWF multimer sizes (N = 10).

Notably, the intersection point of Q_c was not observed in the AVF P2 (Fig 5B). The larger the VWF multimer size was, the higher the SIPAct level. Consequently, larger VWF multimers could pose a higher risk of SIPAct over the investigated range of flow rates in AVF P2.

Fig 3. Key calculated variables in the AVF P1 in systole (upper row) and diastole (lower row). The distributions of the velocity magnitude $|\vec{V}|$ (A), shear stress τ (B), cumulative shear stress CSS (C) and primed platelets P_a (D) are obtained at the highest parameter values (Q^{in}_{av} = 725 mL/min, N = 100). The blue and red colours correspond to the lowest and highest variable values, respectively. The links for the supporting movies are available in S6 Text.

https://doi.org/10.1371/journal.pone.0272342.g003

The results (Fig 5) were approximated by an equation with the following form:

$$PAL = a(Q^{in}_{av} - Q_c)^{\beta} \quad (10)$$

where a, Q_c, and β are approximation parameters. The exponent β was found to be a decreasing function of the VWF multimer size for both patients (Table S6.1 in S6 Text). The obtained result suggests that the SIPAct level for smaller VWF size should exceed the SIPAct level for larger VWF size with an increasing flow rate in AVF P2. In this regard, the point of Q_c seems to lie outside the investigated range of the flow rate (Fig 5B). The abscissa of the curve intersection point (Q_c) was equal to approximately 1585 mL/min for AVF P2. This value exceeds the maximum flow value applied in the simulations (1300 mL/min).

The calculations also indicated that the SIPAct level in AVF P1 is nonzero up to the minimum AVF flow rate (Q^{in}_{av} = 100 mL/min, Fig 5A). In this regard, estimation of the critical flow (Q_{cr}, Eq (10)) was performed via the correlation coefficient maximization method [75]. In turn, the critical flow rates in the case of AVF P2 were obtained via the bisection method. The smaller the multimer size was, the higher the critical flow rate for both AVFs. The founded critical flow rates for the AVFs are presented in S6 Text.

The method is aimed at the calculation of platelet activation level in the vessel of interest using patient-specific biomechanical features as well as the size of von Willebrand factor (VWF) molecules in blood.

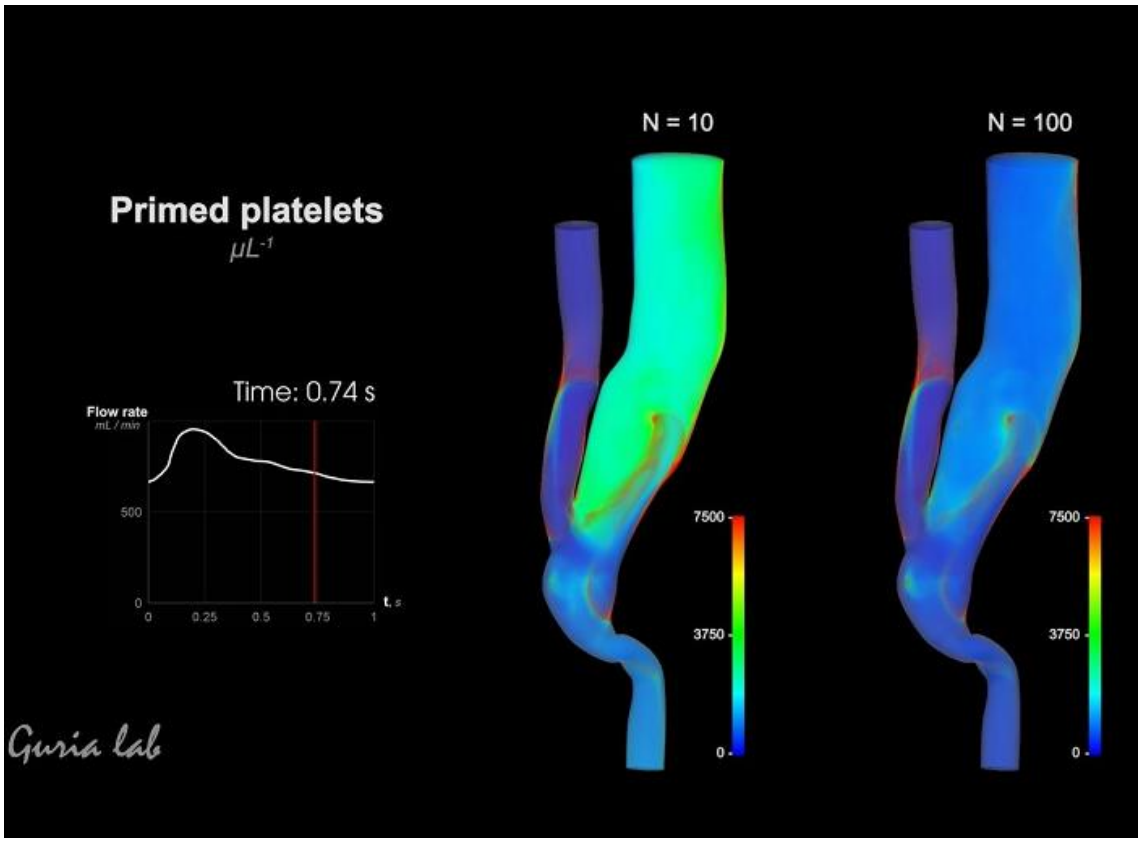

Silicone model of a personalized arteriovenous fistula

A procedure for determining the parametric diagram of platelet activation for patients with haemodialysis arteriovenous fistula have been suggested. The position of critical curves separating activation and non-activation regimes was found to depend on patient-specific factors affecting shear stress distribution in the vessels.

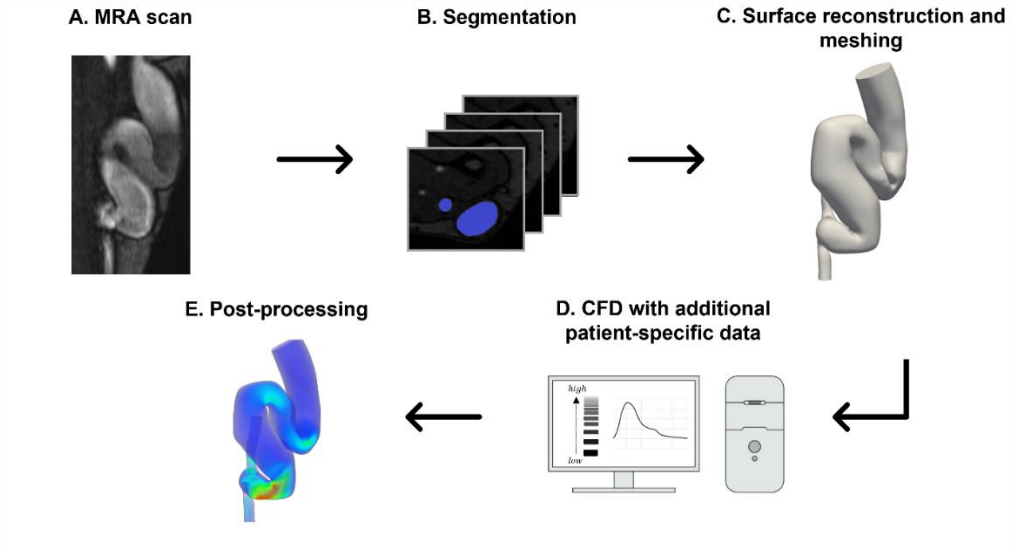

Overview of the platelet activation level estimation in patient-specific large vessels. MRA – magnetic-resonance angiography, CFD – computational fluid dynamics.

The method can be used to compare the impact of biomechanical and biochemical factors on personalized risk of intravascular thrombosis. The developed approach for the analysis of platelet activation risk in specific vessels may serve as an element of a web service for thrombosis diagnostics.

The authors of the work are open for collaboration: guria@blood.ru

The work was supported by Russian Science Foundation (grant No.19-11-00260).